HHS Public Access

Author manuscript

Ceram Int. Author manuscript; available in PMC 2018 October 01.

Published in final edited form as:

Ceram Int. 2017 October 1; 43(14): 10999–11005. doi:10.1016/j.ceramint.2017.05.141.

Speed sintering translucent zirconia for chairside one-visit dental restorations: Optical, mechanical, and wear characteristics

Marina R. Kaizer[a,b], **Petra C. Gierthmuehlen**[c], **Mateus BF dos Santos**[d], **Sergio S. Cava**[b], and **Yu Zhang**[a,*]

[a]Department of Biomaterials and Biomimetics, New York University College of Dentistry, New York, NY 10010, USA

[b]Graduate Program in Materials Science and Engineering, Federal University of Pelotas, Pelotas, Brazil

[c]Department of Prosthodontics, University Medical Center Duesseldorf, Moorenstrasse 5, 40225 Duesseldorf, Germany

[d]Graduate Program in Dentistry, Federal University of Pelotas, Pelotas, Brazil

Abstract

The fabrication of zirconia dental restorations is a time-consuming process due to traditional slow sintering schemes; zirconia (Y-TZP) produced by these conventional routes are predominantly opaque. Novel speed sintering protocols have been developed to meet the demand for time and cost effective chairside CAD/CAM-produced restorations, as well as to control ceramic microstructures for better translucency. Although the speed sintering protocols have already been used to densify dental Y-TZP, the wear properties of these restorations remain elusive. Fast heating and cooling rates, as well as shorter sintering dwell times are known to affect the microstructure and properties of zirconia. Thus, we hypothesize that speed sintered zirconia dental restorations possess distinct wear and physical characteristics relative to their conventionally sintered counterparts. Glazed monolithic molar crowns of translucent Y-TZP (inCoris TZI, Sirona) were fabricated using three distinct sintering profiles: Super-speed (**SS**, 1580 °C, dwell time 10 min), Speed (**S**, 1510 °C, dwell time 25 min), and Long-term (**LT**, 1510 °C, dwell time 120 min). Microstructural, optical and wear properties were investigated. Crowns that were super-speed sintered possessed higher translucency. Areas of mild and severe wear were observed on the zirconia surface in all groups. Micropits in the wear crater were less frequent for the LT group. Groups **S** and **SS** exhibited more surface pits, which caused a scratched steatite surface that is associated with a greater volume loss. Tetragonal to monoclinic phase transformation, resulting from the sliding wear process, was present in all three groups. Although all test groups had withstood thermo-mechanical challenges, the presence of hairline cracks emanating from the

*Correspondence to: Department of Biomaterials and Biomimetics, New York University College of Dentistry, 433 First Avenue, Room 810, New York, NY 10010, USA. yz21@nyu.edu (Y. Zhang).

Conflict of interest: All authors declare no conflict of interest.

occlusal wear facets and extending deep into the restoration indicates their susceptibility to fatigue sliding contact fracture.

Keywords

Y-TZP; Monolithic zirconia; Speed sintering; Translucency; Mechanical properties; Wear resistance

1. Introduction

Full-contour monolithic zirconia crowns are increasingly used in prosthetic dentistry because of their strength, resistance to fracture, and fabrication simplicity [1–3]. Although only some preliminary clinical trials on monolithic zirconia dental restorations have been published [1,4–7], in vitro studies revealed that monolithic zirconia crowns can endure the highest fracture load among all ceramic restorative systems [3,8]. In addition, laboratory testing [9–12] and clinical researches [5,13,14] have shown that polished zirconia causes less tooth enamel wear than glazed zirconia, whereas glazed zirconia exhibits comparable or better results than other dental ceramic materials.

Monolithic zirconia dental restorations are produced from a some-what translucent, strong and dense zirconia. These desirable properties can be obtained by manipulating sintering additives and conditions. The elimination of light-scattering alumina sintering aids and porosities improves translucency, but requires a higher sintering temperature (1530 °C) in conjunction with a longer dwell time (6 h) [8]. Reducing the grain size and increasing the green compact density also improves translucency. In this case, a lower sintering temperature (1450 °C) and shorter dwell time (2 h) are necessary [8]. A further increase in translucency can be achieved by keeping zirconia grain size under 100 nm while eliminating defects such as pores and oxygen vacancies [15]. Such a microstructure would allow light transmission without substantial scattering, yielding a translucency similar to that of dental porcelains. To date, it is still challenging to densify Y-TZP with a sub-100 nm grain size. Speed sintering is one of the plausible routes to produce dense, ultrafine-grained Y-TZP.

Traditionally, the sintering of Y-TZP for engineering applications is a time consuming process, which involves a ‘slow’ heating and cooling rate (typically 5 – 10 °C per minute) coupled with a prolonged dwell time (often amounting to several hours). The resulting materials are strong but largely opaque. Dentistry is now redefining protocols for ultrafast ceramic sintering. Novel speed and super-speed sintering protocols have been developed [16] to meet the demand for time and cost effective chairside one-visit CAD/CAM-produced restorations, as well as to prevent Y-TZP grain growth for better translucency. The effect of speed sintering on the flexural strength of monolithic Y-TZP has been investigated [16], showing that no significant difference was observed in the flexural strength of Y-TZP when speed sintered with a dwell time of 25 min at 1540 °C (σ=622.3 ± 82.7 MPa) and conventionally sintered with a dwell time of 120 min at 1510 °C (σ=579.7± 130.6 MPa). However, when super-speed heating and cooling rates, as well as a short dwell time, were used (the sample was placed in a 1580 °C pre-heated furnace and removed after 10 min dwell time), the flexural strength achieved was much higher (904 ± 115.7 MPa). It is unclear

why super-speed sintering may lead to a superior flexural strength in Y-TZP; such a phenomenon appears to defy the theory of thermal stress resistance of ceramics. Nevertheless, speed and super-speed sintered dental zirconia are already in the market, and likely in patients' mouths, although their fatigue and wear properties remain elusive. To the best of our knowledge, nothing has yet been published on how speed sintering of monolithic zirconia dental restorations would affect its microstructure, translucency, and wear characteristics.

2. Experiment

2.1. Specimen preparation

The monolithic translucent zirconia molar crowns (inCoris TZI, Sirona) tested herein were CAD/CAM-milled, sintered and glazed by Sirona. Sintering was carried out according to the following protocols:

- Long-term sintering (**LT**): served as a reference group: heating at 25 °C/min to 800 °C, then at 15 °C/min to 1510 °C, dwelling for 120 min, followed by cooling at 30 °C/min down to 200 °C before
- removing from the furnace. Total sintering time 4 h. Speed sintering (**S**): heating at 99 °C/min to 1100 °C, then at 50 °C/min to 1510 °C, dwelling for 30 min, followed by cooling at 99 °C/ min down to 800 °C dwelling for 5 min before removing from the
- furnace. Total sintering time 60 min. Super-speed sintering (**SS**): Crown is placed in a pre-heated furnace at 1580 °C, dwelling for 10 min, and immediately removed from the furnace. Total sintering time 10 min.

2.2. Microstructure

One crown per group was polished to a flat surface with a 1 μm diamond suspension finish, and then thermally etched at 1150 °C for 20 min with a heating and cool rate of 40 °C/min. Imaging was performed in a scanning electron microscope (Hitachi 3500 N, Japan). The zirconia grain size was measured using the linear intercept method [17].

2.3. Physical properties

The translucency of the crown buccal wall was analyzed using a colorimeter (SpectroShade™Micro, MHT Optic Research AG, Switzerland), operating in the CIE L^* a^* b^* system. Variations in thickness of the buccal wall are expected due to the anatomic contours, resulting in an overall thickness of 2.3 ± 0.24 mm. Nevertheless, the average buccal thickness across the specimens in each group were: SS = 2.3 ± 0.02 mm, **S** = 2.3 ± 0.03 mm, **LT** = 2.3 ± 0.02 mm, suggesting that translucency was measured under very similar conditions within and across groups. The translucency parameter (TP) was calculated using the following equation:

$$TP=(\left(L_W^*-L_B^*\right)^2+\left(a_W^*-a_B^*\right)^2+\left(b_W^*-b_B^*\right)^2)^{1/2} \quad (1)$$

where the subscripts W and B refer to color coordinates with the white and black background, respectively [18]. All zirconia crowns were fabricated with the same crown design given by the CAD/CAM system, thus fitted on an identical die. This aspect made possible to use standard dies, one white (L^* = 1.8, a^* = 1.3, b^* = −1.5) and one black (L^* = 95.7, a^* = −1.3, b^* = 2.6), as backgrounds for the translucency readings of all crowns.

The hardness of the three test groups was measured on polished surfaces (1 μm diamond grits) using a Vickers hardness tester at a peak load of 10 N with a holding time of 15 s.

2.4. Sliding wear test

For wear testing, crowns were cemented to aged (stored in distilled water at 37 °C for 3–5 weeks) resin-based composite dies (Tetric Evo Ceram, Ivoclar Vivadent, Liechtenstein) with a resin-based dental luting material (Multilink Automix, Ivoclar) following the manufacturer's recommendations. After cementation, specimens were stored in water for 5–10 days prior to sliding wear testing to allow hydration of the resin cement.

Crowns (n = 10) were subjected to sliding wear testing in water using a chewing simulator (Willytec, Germany) with load application of 198 N for 1.2 million cycles at a frequency of 1.6 Hz. Simulated chewing was set up using the following parameters: vertical movement 6 mm, horizontal movement 0.5 mm, descending speed 60 mm/s, rising speed 55 mm/s, forward speed 60 mm/s, backward speed 55 mm/s. Sliding wear testing was performed with a spherical steatite indenter as the antagonist (Hoechst Ceram Tec, Germany, r = 3 mm), sliding down the mesio-lingual cusp towards the central fossa. During cyclic loading, all samples were simultaneously exposed to thermal cycling in water at 5 and 55 °C at intervals of 60 s.

2.5. Analyzes of wear damage sustained by both the zirconia crowns and antagonists

Wear depth and volume loss were not quantified for the zirconia crowns because the material loss was predominantly contributed from the removal of the glaze layer, with only minor superficial damage to the zirconia. Therefore, the measurements would only represent variations of the glaze layer thickness rather than actual differences among test groups. On the other hand, the wear of the antagonists was due mainly to sliding contact with the exposed zirconia surface. The glaze material was worn out as soon as 500 cycles, causing negligible wear on the antagonists. Thus, differences among the three Y-TZP groups could potentially affect the wear behavior of the antagonist [5,13,19]. Quantitative analysis of wear depth and volume loss for the steatite antagonists were carried out on 3D images obtained by a micro computed tomography scanner (micro-CT Scanco 40 medical AG, Bassersdorft, Switzerland). The scanner operated in high resolution (Voxel size: 8 μm), at 70kVp energy, intensity of 114 μA (0.5 mm AL Filter), and integration time 250 ms. The micro-CT slices were assembled as 3D models using a medical image processing software (Mimics Research 17.0, Materialise, Belgium) and exported as stereolithography (stl) files to a specific

software for 3D metrology (Geomagic Qualify 2013. 3D Systems, USA). The original spherical topography of each steatite ball was reconstructed by means of mesh editing. The same 3D models were compared before and after topographical reconstruction to determine the maximum wear depth and volume loss.

Qualitative analysis of the damage sustained in both zirconia crowns and steatite antagonists following 1.2 million sliding cycles at 198 N was performed using optical and scanning electron microscopes (SEM). Representative crowns were first imaged for occlusal surface damage associated with the wear crater and its surrounding areas using optical and SEM microscopies. The crowns were then embedded in clear epoxy resin and sectioned for subsurface damage evaluations. Sectioning took place along the direction of sliding contact and slightly away from the center of the wear crater, using a water cooled low speed diamond saw (Isomet, Buehler, Lake Buff, IL). The cross-sections were polished up to the center of the wear crater with a 1 μm diamond suspension finish and analyzed in the SEM for the presence of cracks and fractures.

The zirconia phase contents on the surface of the wear crater was assessed using a micro-XRD equipped with a VANTEC-2000 area detector (D8 Discover Gadds microdiffractometer, Bruker, USA). The X-ray generated from a sealed Cu tube was monochromated by a graphite crystal and collimated by a 0.05 mm MONOCAP (λ Cu-Kα = 1.54178 Å). An area of 50 μm (diameter) in the center of the wear crater was analyzed based on the spectra collected between 25° and 35° 2θ. The zirconia phase contents of a control area (not exposed to wear), gently polished to remove its glaze layer, was also analyzed on the same crown.

2.6. Statistical analyses

The translucency parameter and Vickers hardness data were analyzed using One Way ANOVA. Wear depth and volume loss data were heterocedastic, thus analyzed using One Way ANOVA on Ranks. All pairwise multiple comparisons were performed by using the Tukey Test. The significance level was set at 5%.

3. Results and discussion

The wear behavior of the translucent monolithic zirconia for chairside one-visit dental restorations was investigated in the present study. The wear behavior of materials can be affected by the material type, microstructure, and physical properties [11,20–22]. For zirconia, the sintering conditions play an important role in microstructure and physical properties [23–27].

For microstructural analyses, Y-TZP specimens were fine-polished and thermally etched prior to SEM examination. The thermal etching temperature employed was much lower than those typically indicated for the thermal etching of ceramics (i.e. 50 – 100 °C lower than the sintering temperature). To prevent any grain growth, the lowest temperature possible to achieve the thermal etching of the Y-TZP surface was determined. Tests started at 900 °C with a dwell time of 20 min, increasing 50 °C with each trial, until the temperature of 1150 °C was reached and adequate thermal etching was obtained (see Fig. 1). Considering

that the biscuit sintering temperature for most dental Y-TZP ranges between 1100 °C and 1200 °C, one can assume that the current thermal etching process would not cause any grain growth. There are two important aspects here: (1) The new translucent zirconia materials possess a fine-grained microstructure; therefore, the thermal etching protocols, as well as any post-sintering thermal treatment protocols, should be carefully revised; (2) The calibration and accuracy of the furnaces used for sintering and post-sintering thermal treatments have to be carefully controlled, as the suggested protocols are highly sensitive to deviations in sintering parameters.

The microstructure of the three zirconia test groups is shown in Fig. 1. Fig. 1a features a pattern of larger grains consisting of clusters of smaller grains, regardless of the zirconia group. Images in Fig. 1b are high magnification depictions of the micropits on the Y-TZP surfaces induced from the wear test, where some of the surfaces presented exposed grain facets untouched by the antagonist. The size of the exposed grains (Fig. 1b) was similar to that of the larger grains in the thermally etched surfaces (Fig. 1a). Thus, for grain size measurements, the bigger grain boundaries were considered when counting the linear intercepts. The rank of the grain size by group was **LT** > **SS** > **S** (Table 1), indicating that both higher sintering temperature and longer dwell time increased grain growth. These findings are in accordance with previous studies [23–27].

Sintering conditions can also influence the translucency and hardness of ceramics. The translucency of ceramic materials is usually measured in flat specimens of standardized thickness. This approach can be more accurate in determining transmittance, since important factors like thickness and surface quality can be standardized. In the present study, translucency was measured by using the Translucency Parameter method [18], allowing the use of crowns in their final “ready-to-cement” stage. This is more clinically relevant than metallographically polished plates. Similarly, the light transmission through the buccal surface of the crowns has been previously measured by Beuer et al. [20]. It is known that sintering temperature and dwell time affect the density and grain size of ceramics [24,27], therefore affecting translucency [15,24,25,27]. In the present study, relatively low values of translucency were observed for all three sintering protocols tested, with a slightly better performance of the **SS** group (Table 1). However, the **SS** and **S** groups exhibited a slightly lower hardness value relative to group **LT**, due probably to a larger grain size observed in group **LT** [28].

The surface views of wear craters for zirconia and steatite are shown in Fig. 2. Images in Fig. 2a show that the glazing layer has been completely removed, exposing the underlying zirconia in the wear crater. Images in Fig. 2b represent the center of the wear crater on zirconia worn surfaces, showing that the **LT** group presents least pit formation. Micropitting is caused by the presence of shallow lateral cracks beneath the wear surface, which can propagate parallel to but eventually intersect with the wear surface, leading to the dislodgement of flakes of zirconia [29]. In addition, micropits were mainly present around the center of the crater where the maximum load is achieved during sliding. The zirconia fragments dislodged during micropit formation act as third body in the wear process, as one can hypothesize associating the findings from Fig. 2b and d: groups **S** and **SS** generated more fragments of zirconia during the cyclic sliding contact process, since these groups

presented more micropits on their surfaces than the group **LT**. Consequently, the antagonistic steatite surfaces for groups **S** and **SS** contained more scratch marks due to the presence of zirconia fragments. In addition, greater volume loss and wear depth were measured in the antagonist for groups **S** and **SS** relative to **LT** (Table 2).

Two distinct patterns of zirconia superficial microdamage were identified after the sliding wear test (Fig. 3): mild wear and severe wear surfaces [30]. Mild wear areas exhibited a smooth surface with a smeared appearance (Fig. 3c). Cumulative damage led to zirconia grain dislodgment, resulting in the severe wear region with a rough surface feature (Fig. 3d). The severe wear areas were frequently associated with cracks that would either evolve to deep penetrating partial cone cracks [26] or to shallow lateral cracks that lead to the spalling of a smeared zirconia layer and creating micropits with exposed grain facets [29].

Ideally, a ceramic dental prosthesis should not surpass a mild wear condition in long-term clinical service. This requirement is the minimum criterion to prevent sliding contact fracture. Whereas the use of a high-toughness material, like zirconia, should ensure high resistance to sliding contact fracture, such advantage can quickly diminish if the friction at the interface of the two contacting bodies is high due to severe wear [26]. In the present study, the presence of partial cone cracks (Fig. 4) emanating from the occlusal wear facets and extending deep into the restoration indicates susceptibility to sliding contact fracture. For the three groups, the dominant crack is located around half way along the sliding track (Fig. 4a), which corresponds to the maximum load area during sliding. The depths measured for the dominant cracks presented in Fig. 4 are: **LT** – 250 μm, **S** – 160 μm, **SS** – 110 μm. Note that it was not possible to show the full length of those hairline cracks (Fig. 4b), because they were not visible in a lower magnification necessary to include their full length. Besides the dominant crack, groups **S** and **SS** also present other cracks throughout the sliding track. These cracks formed at lower loads, before or after the maximum load was reached, were not observed for the **LT** group.

The results of the present study showed the phase transformation of zirconia (Fig. 5) from tetragonal to monoclinic at the surface of the wear crater, which is a direct response to the cyclic sliding contact causing hydrothermal degradation [31,32]. The crack propagation associated with cyclic sliding contact, in warm and wet environments, is in part due to moisture-assisted slow crack growth. However, more deleterious for crack propagation are the mechanical processes such as hydraulic pumping and internal friction at the crack walls [33]. These mechanical fatigue mechanisms are dependent only on the number of cycles, and its behavior indicates a sustained driving force throughout the entire crack evolution [34–40]. From the clinical standpoint, when the restoration is in occlusal function, the cumulative chewing cycles would be the cause of such mechanical fatigue mechanisms, providing a persistent driving force for crack propagation and eventually leading to the fracture of ceramic structures. However, considering the monolithic ceramics available, zirconia remains the most robust of them all [8].

4. Summary

Distinct wear behaviors have been observed among the zirconia crowns fabricated using different sintering protocols, which dictate their microstructure. Fast sintering protocols yield promising results in terms of microstructural, physical and wear properties of monolithic zirconia restorations. However, the wear of the antagonist seemed to be poorer with fast sintered zirconia; thus, further investigation is advised. Although zirconia has been perceived as the most robust ceramic restorative material, the presence of hairline cracks emanating from the occlusal wear facets and extending deep into the restoration, as well as the phase transformation associated with the wear process, indicate the susceptibility of zirconia ceramics to sliding contact fracture.

Acknowledgments

Funding was provided by the United States National Institute of Dental and Craniofacial Research (Grants 2R01 DE017925 and 1R01 DE026772) and the National Science Foundation (Grant CMMI-0758530). The authors would like to thank Sirona for fabricating the zirconia crowns and Mrs. Iris Walz for performing the fatigue test.

References

1. Lohbauer U, Reich S. Antagonist wear of monolithic zirconia crowns after 2 years. Clin Oral Investig. 2016
2. Sulaiman TA, Abdulmajeed AA, Donovan TE, Cooper LF, Walter R. Fracture rate of monolithic zirconia restorations up to 5 years: a dental laboratory survey. J Prosthet Dent. 2016; 116:436–439. [PubMed: 27178771]
3. Zhang Y, Mai Z, Barani A, Bush M, Lawn B. Fracture-resistant monolithic dental crowns. Dent Mater. 2016; 32:442–449. [PubMed: 26792623]
4. Batson ER, Cooper LF, Duqum I, Mendonca G. Clinical outcomes of three different crown systems with CAD/CAM technology. J Prosthet Dent. 2014; 112:770–777. [PubMed: 24980739]
5. Mundhe K, Jain V, Pruthi G, Shah N. Clinical study to evaluate the wear of natural enamel antagonist to zirconia and metal ceramic crowns. J Prosthet Dent. 2015; 114:358–363. [PubMed: 25985742]
6. Stober T, Bermejo JL, Schwindling FS, Schmitter M. Clinical assessment of enamel wear caused by monolithic zirconia crowns. J Oral Rehabil. 2016; 43:621–629. [PubMed: 27198539]
7. Bomicke W, Rammelsberg P, Stober T, Schmitter M. Short-term prospective clinical evaluation of monolithic and partially veneered zirconia single crowns. J Esthet Restor Dent. 2016
8. Zhang Y, Lee JJ, Srikanth R, Lawn BR. Edge chipping and flexural resistance of monolithic ceramics. Dent Mater. 2013; 29:1201–1208. [PubMed: 24139756]
9. Burgess JO, Janyavula S, Lawson NC, Lucas TJ, Cakir D. Enamel wear opposing polished and aged zirconia. Oper Dent. 2014; 39:189–194. [PubMed: 23848069]
10. Janyavula S, Lawson N, Cakir D, Beck P, Ramp LC, Burgess JO. The wear of polished and glazed zirconia against enamel. J Prosthet Dent. 2013; 109:22–29. [PubMed: 23328193]
11. Park JH, Park S, Lee K, Yun KD, Lim HP. Antagonist wear of three CAD/CAM anatomic contour zirconia ceramics. J Prosthet Dent. 2014; 111:20–29. [PubMed: 24199603]
12. Stawarczyk B, Ozcan M, Schmutz F, Trottmann A, Roos M, Hammerle CHF. Two-body wear of monolithic, veneered and glazed zirconia and their corresponding enamel antagonists. Acta Odontol Scand. 2013; 71:102–112. [PubMed: 22364372]
13. Esquivel-Upshaw JF, Rose WF Jr, Barrett AA, Oliveira ER, Yang MC, Clark AE, Anusavice KJ. Three years in vivo wear: core-ceramic, veneers, and enamel antagonists. Dent Mater. 2012; 28:615–621. [PubMed: 22410113]

14. Suputtamongkol K, Anusavice KJ, Suchatlampong C, Sithiamnuai P, Tulapornchai C. Clinical performance and wear characteristics of veneered lithia-disilicate-based ceramic crowns. Dent Mater. 2008; 24:667–673. [PubMed: 17727943]
15. Zhang Y. Making yttria-stabilized tetragonal zirconia translucent. Dent Mater. 2014; 30:1195–1203. [PubMed: 25193781]
16. Ersoy NM, Aydoğdu HM, Değirmenci BÜ, Çökük N, Sevimay M. The effects of sintering temperature and duration on the flexural strength and grain size of zirconia. Acta Biomater Odontol Scand. 2015; 1:43–50. [PubMed: 28642900]
17. Wurst JC, Nelson JA. Lineal intercept technique for measuring grain size in two- phase polycrystalline ceramics. J Am Ceram Soc. 1972; 55:109–109.
18. Shiraishi T, Wood DJ, Shinozaki N, van Noort R. Optical properties of base dentin ceramics for all-ceramic restorations. Dent Mater. 2011; 27:165–172. [PubMed: 21055800]
19. Etman MK, Woolford M, Dunne S. Quantitative measurement of tooth and ceramic wear: in vivo study. Int J Prosthodont. 2008; 21:245–252. [PubMed: 18548965]
20. Beuer F, Stimmelmayr M, Gueth JF, Edelhoff D, Naumann M. In vitro performance of full-contour zirconia single crowns. Dent Mater. 2012; 28:449–456. [PubMed: 22196898]
21. Heintze SD, Cavalleri A, Forjanic M, Zellweger G, Rousson V. Wear of ceramic and antagonist–a systematic evaluation of influencing factors in vitro. Dent Mater. 2008; 24:433–449. [PubMed: 17720238]
22. Sabrah AH, Cook NB, Luangruangrong P, Hara AT, Bottino MC. Full-contour, Y-TZP ceramic surface roughness effect on synthetic hydroxyapatite wear. Dent Mater. 2013; 29:666–673. [PubMed: 23566765]
23. Inokoshi M, Zhang F, De Munck J, Minakuchi S, Naert I, Vleugels J, Van Meerbeek B, Vanmeensel K. Influence of sintering conditions on low-temperature degradation of dental zirconia. Dent Mater. 2014; 30:669–678. [PubMed: 24698437]
24. Jiang L, Liao Y, Wan Q, Li W. Effects of sintering temperature and particle size on the translucency of zirconium dioxide dental ceramic. J Mater Sci Mater Med. 2011; 22:2429–2435. [PubMed: 21922331]
25. Kim MJ, Ahn JS, Kim JH, Kim HY, Kim WC. Effects of the sintering conditions of dental zirconia ceramics on the grain size and translucency. J Adv Prosthodont. 2013; 5:161–166. [PubMed: 23755342]
26. Ren L, Zhang Y. Sliding contact fracture of dental ceramics: principles and validation. Acta Biomater. 2014; 10:3243–3253. [PubMed: 24632538]
27. Stawarczyk B, Ozcan M, Hallmann L, Ender A, Mehl A, Hammerlet CH. The effect of zirconia sintering temperature on flexural strength, grain size, and contrast ratio. Clin Oral Investig. 2013; 17:269–274.
28. Zhang Y, Cheng YB. Microstructural design of Ca alpha-sialon ceramics: effects of starting compositions and processing conditions. J Eur Ceram Soc. 2003; 23:1531–1541.
29. Zhang Y, Cheng YB, Lathabai S. Influence of microstructure on the erosive wear behaviour of Ca - sialon materials. J Eur Ceram Soc. 2001; 21:2435–2445.
30. Zhang Y, Cheng YB, Lathabai S. Erosion of alumina ceramics by air- and water- suspended garnet particles. Wear. 2000; 240:40–51.
31. Denry I, Kelly JR. State of the art of zirconia for dental applications. Dent Mater. 2008; 24:299–307. [PubMed: 17659331]
32. Kim JW, Covel NS, Guess PC, Rekow ED, Zhang Y. Concerns of hydrothermal degradation in CAD/CAM zirconia. J Dent Res. 2010; 89:91–95. [PubMed: 19966039]
33. Zhang Y, Sailer I, Lawn BR. Fatigue of dental ceramics. J Dent. 2013; 41:1135–1147. [PubMed: 24135295]
34. Bhowmick S, Zhang Y, Lawn BR. Competing fracture modes in brittle materials subject to concentrated cyclic loading in liquid environments: bilayer structures. J Mater Res. 2005; 20:2792–2800.
35. Hermann I, Bhowmick S, Zhang Y, Lawn BR. Competing fracture modes in brittle materials subject to concentrated cyclic loading in liquid environments: trilayer structures. J Mater Res. 2006; 21:512–521.

36. Kim JW, Kim JH, Thompson VP, Zhang Y. Sliding contact fatigue damage in layered ceramic structures. J Dent Res. 2007; 86:1046–1050. [PubMed: 17959894]
37. Zhang Y, Bhowmick S, Lawn BR. Competing fracture modes in brittle materials subject to concentrated cyclic loading in liquid environments: monoliths. J Mater Res. 2005; 20:2021–2029.
38. Zhang Y, Kim JW. Graded zirconia glass for resistance to veneer fracture. J Dent Res. 2010; 89:1057–1062. [PubMed: 20651092]
39. Zhang Y, Kim JW, Kim JH, Lawn BR. Fatigue damage in ceramic coatings from cyclic contact loading with a tangential component. J Am Ceram Soc. 2008; 91:198–202.
40. Zhang Y, Song JK, Lawn BR. Deep-penetrating conical cracks in brittle layers from hydraulic cyclic contact. J Biomed Mater Res B Appl Biomater. 2005; 73:186–193. [PubMed: 15672403]

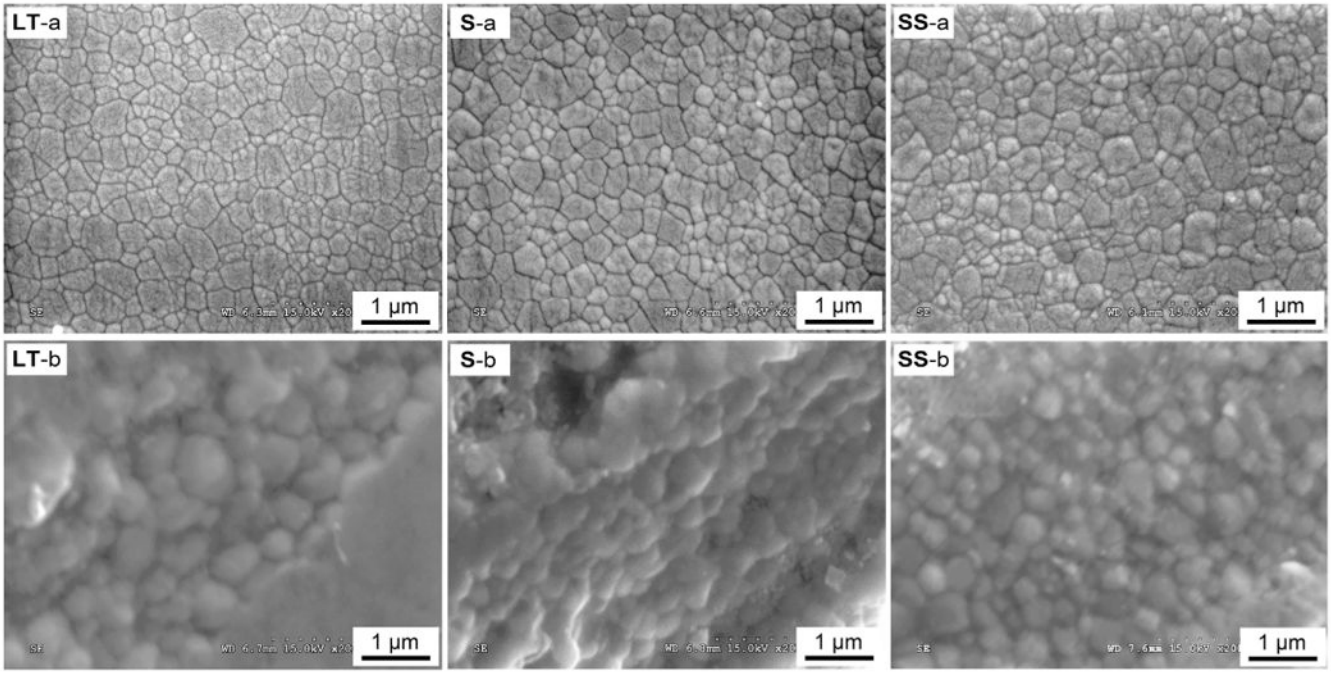

Fig. 1.

Microstructure of the three zirconia groups (**LT**: Long-term, **S**: Speed, and **SS**: Super-speed). (a) Microstructure after polishing and thermal etching, and (b) Exposed grain facets in the wear micropits.

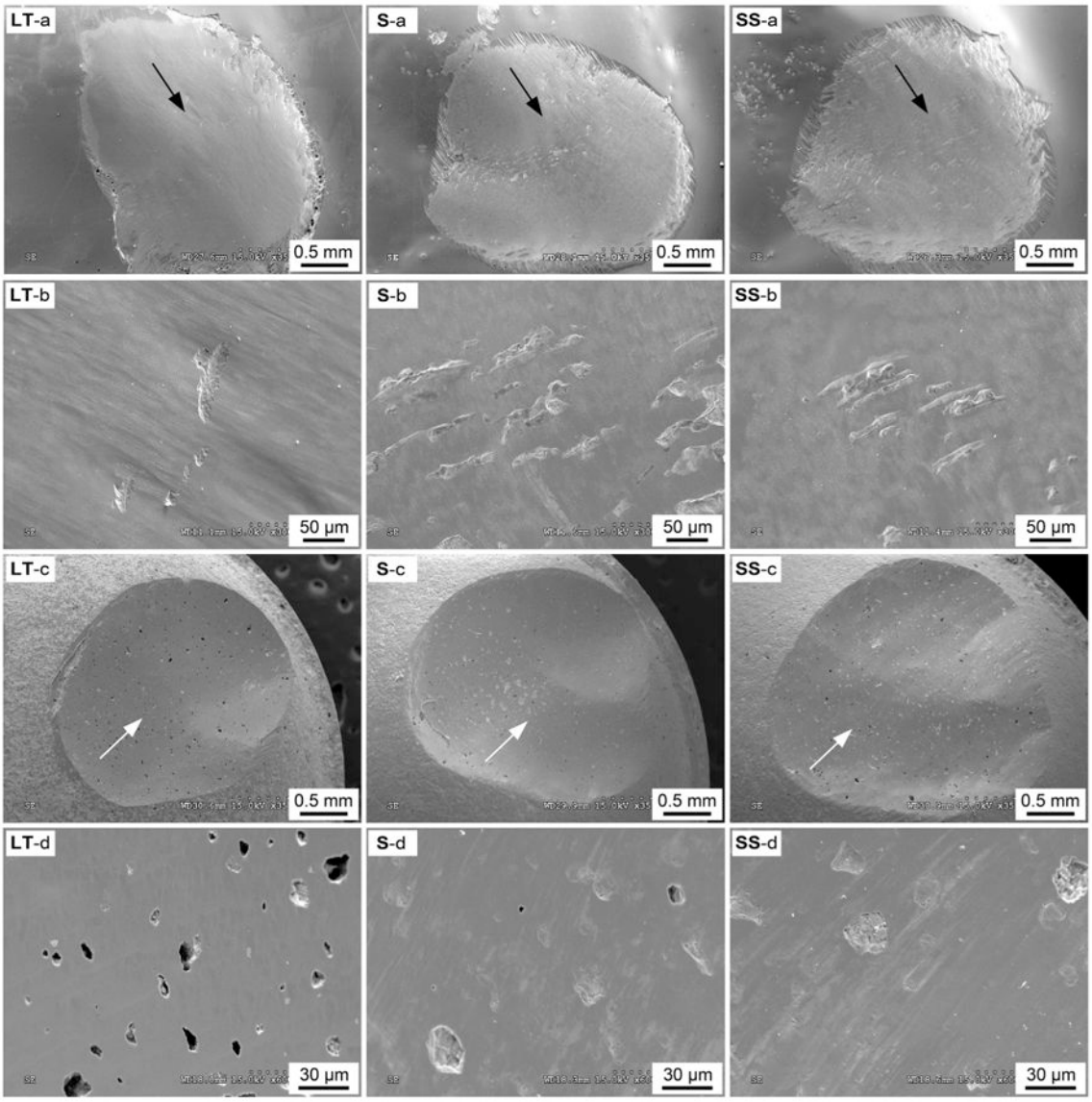

Fig. 2.

SEM images of zirconia and steatite wear crater: (LT) Long-term, (**S**) Speed, (**SS**) Super-speed. General view of the wear craters in (a) zirconia crowns and (c) steatite antagonists. Arrows indicate sliding direction. Surface features at the center of the crater for (b) zirconia crowns and (d) steatite antagonists.

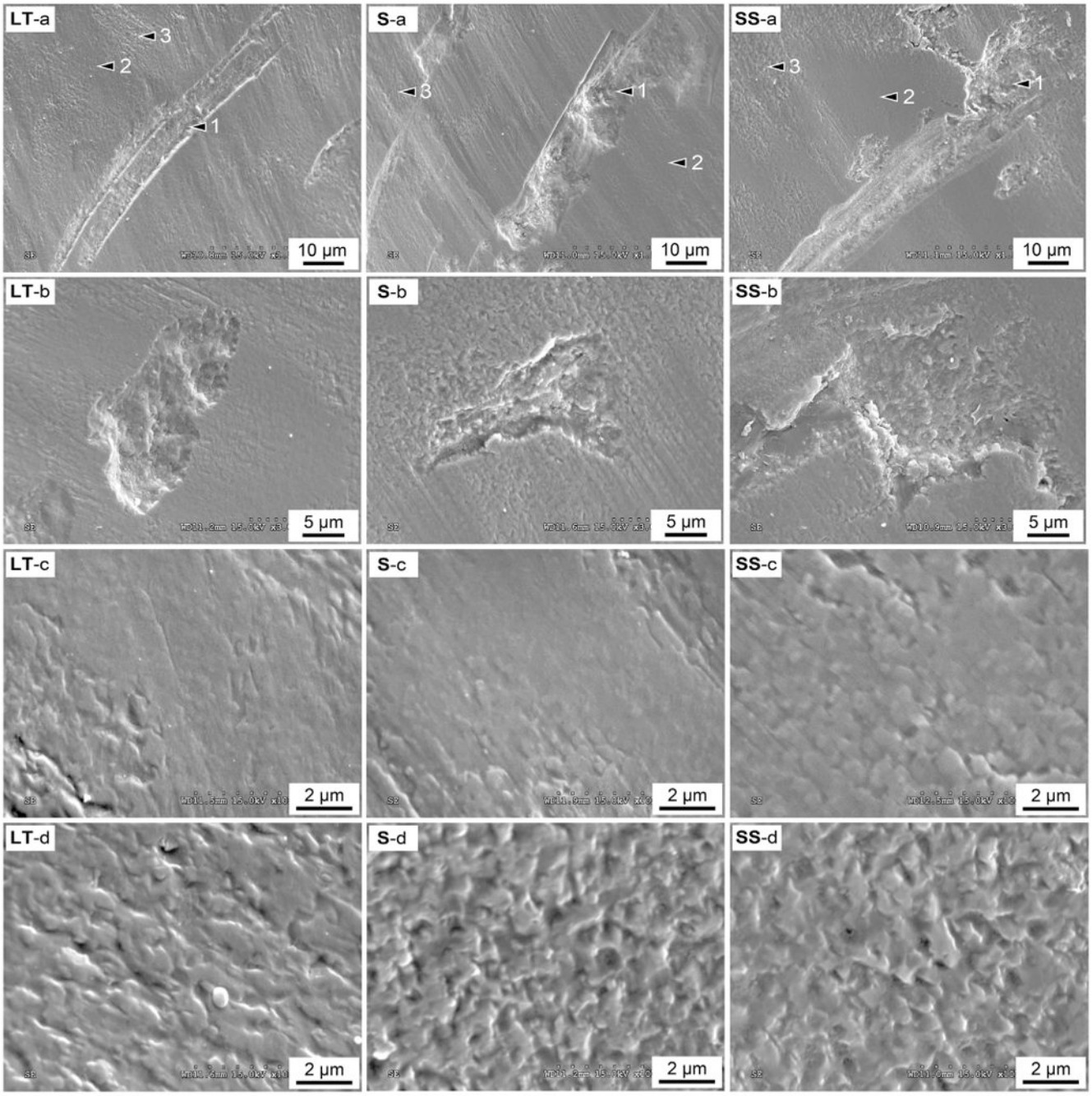

Fig. 3.

Damage sustained in the zirconia surface after sliding wear test: (**LT**) Long-term, (**S**) Speed, (**SS**) Super-speed. (a) 1 – Micropits originated from lateral cracks, 2 – Mild wear surfaces, and 3 – Severe wear surfaces with grain dislodgment. High magnification views of (b) micropits, (c) the smooth mild wear surfaces, and (d) the rough severe wear surfaces.

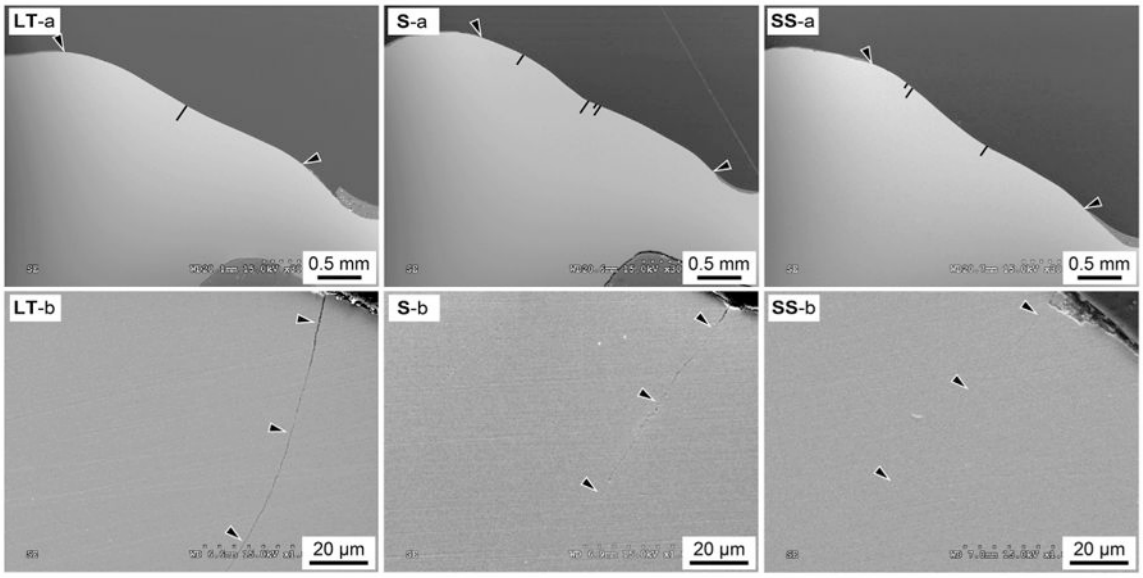

Fig. 4.

Crack distribution and morphology in the zirconia wear craters (**LT**: Long-term, **S**: Speed, and **SS**: Super-speed). (a) Cross-section of representative crowns – arrows indicate the top and bottom boundaries of a wear crater and black lines indicate the location and length of cracks. (b) Cross-sectional view of the dominant partial cone crack.

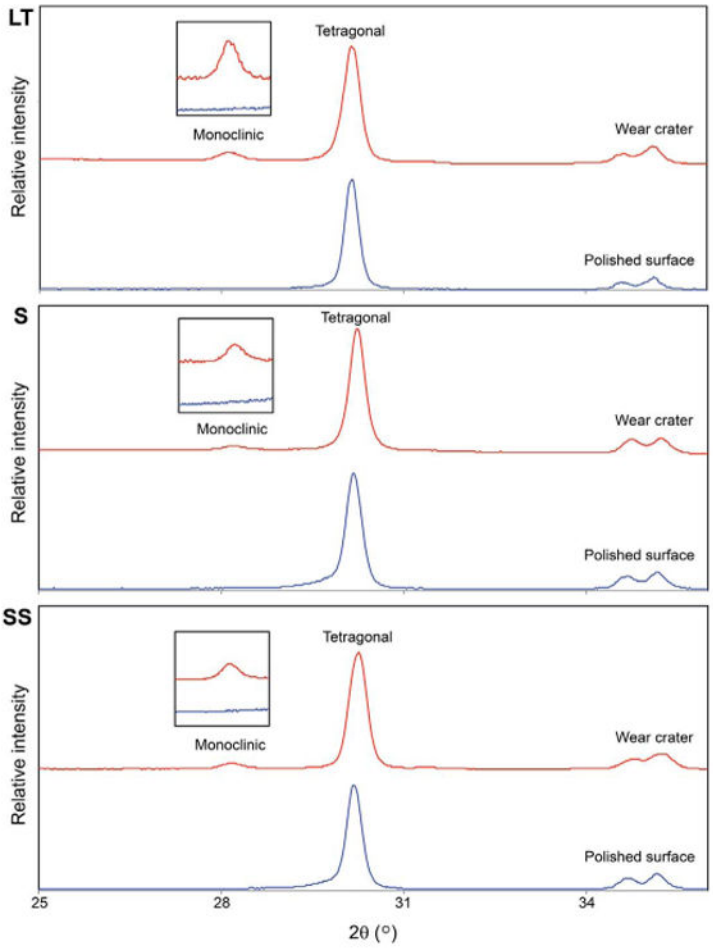

Fig. 5.

Micro XRD spectra comparing the worn and control surfaces of the three zirconia groups tested.

Table 1

Optical and mechanical properties of the zirconias tested, showing mean (standard deviation) for grain size (D), translucency (TP), hardness (HV), and flexural strength (σ)*.

	SS	S	LT
D (μm)	0.59	0.50	0.66
TP	4.6 (0.4)[a]	4.2 (0.5)[b]	4.3 (0.4)[ab]
HV (GPa)	13.1 (0.2)[b]	13.1 (0.2)[b]	13.3 (0.1)[a]
σ (MPa)*	904.2.7 (115.7)[a]	622.3 (82.7)[b]	579.7 (130.6)[b]

TP and HV data were analyzed using One Way ANOVA and Tukey test (5%), comparing the zirconia groups. Distinct superscript letters within the same row indicate statistical differences among groups.

*The flexural strength data were published by Dr. Ersoy and colleagues in 2015 [16]. Data were obtained using the 3-point bend test with bar specimens of 1.2 × 4 × 25 mm in dimension (n = 20) according to ISO 6872.

Table 2

Quantification of wear of the steatite antagonist, showing medians (25–75%) for wear volume and wear depth.

	LT	S	SS
Wear depth (mm)	0.76 (0.70 – 0.81)[b]	0.63 (0.62 – 0.65)[b]	1.04 (0.93 – 1.14)[a]
Wear volume (mm^3)	1.12 (1.05 – 1.20)[b]	1.42 (1.25 – 1.58)[a]	1.86 (1.58 – 2.15)[a]

Note: Superscript letters within the same row indicate differences among groups. The data for each outcome were heterocedastic, thus analyzed by using One Way ANOVA on Ranks and Tukey test (5%).